HHS Public Access

Author manuscript

Mol Genet Metab. Author manuscript; available in PMC 2018 March 01.

Published in final edited form as:

Mol Genet Metab. 2017 March ; 120(3): 198–206. doi:10.1016/j.ymgme.2016.12.002.

Precision medicine in rare disease: Mechanisms of disparate effects of *N*-carbamyl-L-glutamate on mutant CPS1 enzymes

Dashuang Shi[*], **Gengxiang Zhao**, **Nicholas Ah Mew**, and **Mendel Tuchman**

Center for Genetic Medicine Research, Department of Integrative Systems Biology, Children's Research Institute, Children's National Health System, The George Washington University, Washington, DC 20010, USA

Abstract

This study documents the disparate therapeutic effect of *N*-carbamyl-L-glutamate (NCG) in the activation of two different disease-causing mutants of carbamyl phosphate synthetase 1 (CPS1). We investigated the effects of NCG on purified recombinant wild-type (WT) mouse CPS1 and its human corresponding E1034G (increased ureagenesis on NCG) and M792I (decreased ureagenesis on NCG) mutants. NCG activates WT CPS1 sub-optimally compared to NAG. Similar to NAG, NCG, in combination with MgATP, stabilizes the enzyme, but competes with NAG binding to the enzyme. NCG supplementation activates available E1034G mutant CPS1 molecules not bound to NAG enhancing ureagenesis. Conversely, NCG competes with NAG binding to the scarce M792I mutant enzyme further decreasing residual ureagenesis. These results correlate with the respective patient's response to NCG. Particular caution should be taken in the administration of NCG to patients with hyperammonemia before their molecular bases of their urea cycle disorders is known.

Keywords

N-acetyl-L-glutamate; Hyperammonemia; Carbamyl phosphate synthetase 1 deficiency; Urea cycle disorder; mutations

1. Introduction

Six enzymes and two mitochondrial membrane transporters are involved in the urea cycle of mammals that converts toxic ammonia to urea. Functional deficiency in any of these enzymes or transporters results in hyperammonemia that can cause brain damage, coma, and even death [1]. Carbamyl phosphate synthetase 1 (CPS1) (EC 6.3.4.16), the first and rate limiting enzyme, which is active in the presence of its obligate allosteric activator, *N*-acetyl-L-glutamate (NAG) [2], catalyzing the production of carbamyl phosphate (CP) from ammonium, bicarbonate, and ATP. Therefore, NAG, generated by *N*-acetylglutamate synthase (NAGS), plays a key role in controlling the flux of nitrogen through the urea cycle

[*]Corresponding author at: Center for Genetic Medicine Research, Children's Research Institute, Children's National Health System, 111 Michigan Avenue, N.W., Washington, D.C. 20010-2970, USA, dshi@childrensnational.org (D. Shi).

Conflict of interest

The authors state that there is no conflict of interest.

[3–6]. Clinically and biochemically, CPS1 deficiency (MIM# 237300) is indistinguishable from NAGS deficiency (MIM# 237310), because in both, CPS1 enzyme activity and the urea cycle flux are reduced.

N-carbamyl-L-glutamate (NCG), a deacylase-resistant analog of NAG, can activate CPS1 [7]. Even though *in vitro*, NCG has less than a tenth of the affinity to CPS1 than NAG [8] and activates CPS1 at only about 60% (V_{max}) compared to NAG, patients with NAGS deficiency respond remarkably well to NCG, as evidenced by normalized blood ammonia and restoration of ureagenesis [9–11]. NCG supplementation has also been used successfully in other conditions with hyperammonemia, particularly for the conditions with hypothesized reductions in NAG levels, such as organic acidemias (propionic acidemia [12–19], methylmalonic acidemia [14,20–22] and isovaleric acidemia [23], hyperinsulinism hyperammonemia (HIHA) syndrome [24–26] and valproate-induced hyperammonemia [27–29]). NCG was also used successfully to treat the hyperammonemia caused by mitochondrial carbonic anhydrase VA deficiency [30]. Because of its low toxicity and significant enhancement of ureagenesis in several metabolic disorders [31,32], a therapeutic trial with NCG has been proposed in any patient with undiagnosed hyperammonemia [33,34].

Our recent studies revealed that among 5 subjects under investigation, a patient with homozygous E1034G CPS1 mutation (c. 3101A > G) showed marked clinical improvement while on NCG [35]. Conversely, one subject with homozygous M792I (c. 2376 G > C) mutation responded poorly to NCG supplementation.

We therefore sought to understand and perhaps be able to predict the effect of NCG in patients with CPS1 deficiency by studying the wild type and the respective CPS1 mutant proteins *in vitro*. Our results suggest that when NAG concentration is insufficient to activate all CPS1 enzyme molecules, NCG supplementation could activate additional enzyme proteins to enhance ureagenesis as long as the enzyme has significant residual activity. However, if the NAG generated from NAGS is at high enough concentrations to activate tall residual CPS1 molecules the net effect of NCG addition could be a decrease in ureagenesis. Our studies also indicate that in one of the mutant, NCG may have also acted as a chaperone. The study emphasizes that caution should be taken in supplementing NCG to patients with hyperammonemia, and especially for those patients with presumed low residual CPS1 enzyme.

2. Materials and methods

2.1. Case reports

The two subjects of study were both diagnosed with late-onset CPS1 deficiency and were participants in a 3-day NCG trial [35]. During the trial, the subject homozygous for *CPS1* c. 3101A > G (p.E1034G) displayed a marked decrease in ammonia and increase in ureagenesis. After the trial, she was started on NCG therapy at 100 mg/kg/d. She was stable and had no hyperammonemia episodes for 2.5 years on NCG therapy alone. In contrast, the subject homozygous for *CPS1* c.2376G > C (p.M792I) surprisingly exhibited a reduction in urea production [35].

2.2. Protein preparation, expression and purification

Mouse CPS1 cDNA clones (MR222149) were purchased from OriGene (Rockville, Maryland, USA). The coding region for the full-length mature CPS1 was amplified using In-Fusion HD cloning kit (Clontech). The gene was then subcloned into the pFastBac-NH-1 vector, which was derived from the original pFastbac-1 vector provided in the commercial kit (Bac-to-Bac® Baculovirus Expression System; Invitrogen). The pFastBac-NH-1 was reconstructed by adding a thrombin-cutting site and His6-tag upstream of the EcoR1 site in the multiple cloning region. The correct sequence was confirmed using Retrogen DNA sequencing service. The recombinant mature mouse CPS1 wild-type protein and E1034G and M792I mutants with a His6-tag at the N-terminus were expressed in insect cells and purified as described previously [36]. The expressed wild-type CPS1 and the two mutants, E1034G and M792I, were of similar yield and purity (Fig. 1).

2.3. Site-directed mutagenesis

Site-directed mutant DNA sequences encoding E1034G and M792I were created using primers containing the desired mutations and the QuikChange Mutagenesis Kit according to the manufacturer's protocol (Strategene). The mutant DNA sequences were verified by DNA sequencing.

2.4. Enzyme activity assay

CPS1 activity was assayed at 310 K in a 100 μL solution containing 20 mM KCl, 35 mM NH_4HCO_3, 5 mM ATP, 20 mM $MgCl_2$, 5 mM L-ornithine, 20 mM glycyl-glycine, pH 7.4, 0.5 μg human ornithine transcarbamylase (OTC in house) and fixed amount of NCG (10 mM) and/or NAG (1 mM). The reaction was initiated by the addition of purified recombinant enzyme (20 μg) and was stopped by adding equal volume of solution containing 5 mM ^{13}C-citrulline and 30% TCA (v/v) after 10 min reaction. Precipitated protein was removed by micro-centrifugation. The supernatant (10 μL) was analyzed by LC-MS (Agilent). The mobile phase consisted of 92% solvent A (1 mL trifluoroacetic acid in 1 L water) and 8% solvent B (1 mL trifluoroacetic acid in 1 L of 1:9 water/acetonitrile) and the flow rate was 0.6 mL/min. Citrulline, and ^{13}C-citrulline were detected and quantified by selected ion monitoring. The amounts of resulting citrulline were quantified using C^{13}-citrulline as internal standard.

The titration experiments for bicarbonate, ammonium and ATP were performed at concentrations that varied between 0 and 30 mM, NAG titration experiments were carried out with NAG concentration that varied between 0.25 and 1.0 and NCG concentration fixed at 0.0, 10.0 and 30.0 mM, respectively while NCG titration experiments were performed with NCG concentrations that varied in the range of 0.5–30 mM and NAG concentrations fixed at 0.0, 0.1 and 1.0 mM, respectively. All titration data were fit to hyperbolic ($n = 1$) or sigmoidal kinetics ($V = V_{max}[X]^n/([X]^n + K^n)$, where X is the concentration of substrate or activator, V_{max} is maximum activity, K are the K_m values for each substrate or K_a values for activator NAG or NCG, and n is the Hill coefficient, using the program GraphPad Prism.

2.5. Thermal stability assay

Thermal stability assays were performed in a 96-well plate format using a 7900 HT real-time PCR system (Applied Biosystem) to record changes in the fluorescence signal when the temperature was ramped from 298 K to 353 K to monitor thermal unfolding of proteins in the presence of a fluorescent dye, Sypro Orange (Invitrogen), as previously described [37,38]. Wells contained 6 μg of enzyme in 20 mM glycyl-glycine, pH 7.4, 20 mM KCl, 10% glycerol, and 50X SYPRO orange. All measurements were carried out in triplicate.

2.6. Limited proteolysis assay

The recombinant mouse CPS1 was incubated with 0.08 U of elastase at 310 K for 5–30 min in a solution containing 20 mM glycyl-glycine pH 7.4, 10% glycerol, 20 mM KCl, 20 mM $MgCl_2$, and in the presence of 50 mM ATP, 50 mM ATP + 1 mM NAG and 50 mM ATP + 10 mM NCG, respectively. After limited proteolysis, the residual CPS1 activities were measured and the fluorescence was recorded by adding 50X Sypro orange to probe the partially unfolded states of CPS1.

2.7. Docking analysis for E1034G with NCG

To determine whether NCG binds to the E1034G mutant, we carried out the molecular docking study using Autodock 4.0 tools [39]. The NCG structure was generated using the PRODRG2 server [40]. The structure of the E1034G CPS1 was created by mutating Glu1034 to Gly1034 using Coot [41] on the active form CPS1 structure (PDB ID: 5DOU) [42]. An energy grid was built within a cubic box of dimensions 60 × 60 × 60 Å grid points and 0.375 Å spacing using the Autogrid program. The center of the box was set on the center of ligand that was put on the location of the side-chain of the original E1034. The grid points were generated around the cavity left by E1034G mutation to cover the entire potential NCG binding site. The docking simulations were performed using Lamarckian Genetic Algorithm (LCA) with the default docking parameters.

3. Results

3.1. NCG activates CPS1 suboptimally in comparison to NAG

We carried out a detailed comparative characterization of CPS1 in the presence of NAG or NCG (Fig. 2–3 and Table 1). The most significant difference was the 25-fold increase in the NCG concentration required for half-maximal activation of CPS1 compared to the NAG. The K_m for ATP and ammonium exhibited 2- to 3-fold increase in the presence of NCG compared to NAG, while the affinity for bicarbonate was comparable. In all these experiments, the maximal velocities in the presence of NCG were about 30–60% lower than with NAG. It seems that NCG activated CPS1 suboptimally with lower maximal specific activity in comparison to NAG. These results are consistent with previous studies on the isolated CPS from frog liver [43] and purified rat liver CPS1 [8].

3.2. NCG competes with NAG binding

Since the NAGS gene is normal in patients with CPS1 deficiency, the NAG level should be normal as well in these patients. In order to evaluate the potential competition between NAG

and NCG in activation of WT CPS1, NCG titration experiments were performed in the presence and absence of NAG (Fig. 3A). In the presence of the saturating NAG (1.0 mM), the addition of saturating NCG concentration decreased the enzyme specific activity. It appears that when NAG is at saturating concentrations, NCG competes with NAG binding conferring to a portion of CPS1 a suboptimal activation state, resulting in lower specific activity. However, under unsaturated condition (*e.g.* 0.1 mM NAG), the addition of NCG increased the enzyme activity up to approximately 5.0 mM of NCG. Beyond 5 mM, increased supplementation of NCG decreased the enzyme activity. In order to understand better the competitive interaction between NAG and NCG, NAG titration experiments were carried out in the presence of different concentration of NCG (Fig. 3B). The results revealed that there is a crossing point in the NAG titration curves when NCG is added. This crossing point is different for different amounts of NCG. At a concentration lower than the crossing point of NAG (<0.22 mM), the presence of NCG (10 mM) increased specific activity, but at higher concentrations (>0.22 mM) of NAG, the presence of NCG decreased specific activity. These findings explain the mechanism underlying the results of earlier experiments by others, which showed that the activation of CPS1 saturated with NAG was inhibited by NCG [44]. A similar phenomenon was observed for the effects of glycerol on CPS1 activity in the presence or the absence of NAG [36]. It is particularly interesting to note that the crossing point occurred at a lower concentration of NAG (0.16 mM) when NCG concentration increased to 30 mM. Therefore, when NAG concentration is at 0.20 mM, the addition of 10 mM of NCG increased enzymatic activity, but further increasing concentration of NCG to 30 mM decreased the enzyme activity.

3.3. Mild late-onset phenotype of patient with E1034G mutation is consistent with its significant residual activity

Activity assay demonstrated that the E1034G mouse CPS1 mutant has enzymatic activity that is approximately 30–40% of the WT enzyme (Fig. 3C). This result is consistent with the late-onset phenotype of the patient with the same mutation [35].

3.4. Patient with a severe phenotype affected by M792I mutation is consistent with very low residual activity

Activity assay of the recombinant M792I CPS1 mutant indicated that the residual activity is very low at 0.04 ± 0.01 μmol/mg/min, which is consistent with the more severe phenotype of the patient with the same mutation [35].

3.5. NCG effects on the E1034G CPS1 mutant

NCG can activate the mouse CPS1 E1034G mutant, but with activity of about 30–40% lower than WT CPS1, while the affinity of NCG to E1034G CPS1 mutant seems to be similar to the WT enzyme (Fig. 3D).

In order to define the basis for the favorable effect of NCG in this patient, two experiments were performed to look for stability differences between WT and mutant enzyme in the presence and absence of NAG and/or NCG. In the first experiment, the thermal stability of proteins with and without NAG or NCG was monitored by the fall in the activity of the enzyme after incubation at different temperatures (Fig. 4A).

In the second experiment, protection of the two enzymes by NAG or NCG against thermal unfolding were followed by changes in the fluorescence of a dye (Sybro Orange), which was added before temperature ramps (Fig. 4B).

Both experiments demonstrated that both NAG and NCG protect the WT CPS1 and E1034G mutant from thermal unfolding (Fig. 4C and D). However, NAG appears to protect WT CPS1 from thermal unfolding better than NCG while NCG protects the E1034G mutant slightly better than WT CPS1.

3.6. Protection from protease hydrolysis of E1034G mutant

Previous work has demonstrated that the combination of MgATP and NAG protects the enzyme from inactivation by elastase [45–48]. Recent experiment with recombinant human CPS1 confirmed this observation [36]. Our experiment with recombinant mouse CPS1 also indicated that MgATP in combination with NAG or NCG provided protection from attack by elastase for both WT enzyme and E1034G mutant (Fig. 5A–B). The unfolding of the enzymes can be easily detected by the increase of the fluorescence signal when Sybro Orange was added (Fig. 5C–D).

3.7. M792I mutant is a stable protein

Since the activity of M792I mutant is very low and close to the detection limits of the assay, activity based thermal stability assay could not be performed and could only be evaluated by the fluorescence assay. The results indicated that the melting temperature of M792I is similar to WT CPS1 and E1034G mutant (Fig. 5E). Furthermore, NAG or NCG, in combination with MgATP, afforded the M792I mutant similar protection against attack by elastase (Fig. 5F), implying that NAG or NCG could bind to M792I to convert the mutant protein to the active conformation, even though the catalytic site was damaged.

3.8. M792I mutation likely damages the bicarbonate phosphorylation catalytic site

The availability of human CPS1 crystal structures with and without NAG bound provided a reliable modeling of the effect of the M792I mutation [42]. Met792 is part of the L1β17-L1β18 loop (residues 777-793), also termed the T-loop, which is located at the bicarbonate phosphorylation domain (Fig. 6A–B) [42]. In the *apo* form without ligand bound (PDB ID 5DOT), this T-loop is mobile or disordered and its structure could not been traced. However, in the ligand bound form (ADP and NAG bound; PDB 5DOU), this loop becomes fixed, helping to shape the bicarbonate phosphorylation active site. The conformational changes of the T-loop accompanied the corresponding conformational changes of its equivalent T′-loop (residues 1314-1332, L3β15-L3β16 loop) in the carbamate phosphorylation domain L3. Similarly, the T′-loop helped to shape the carbamate phosphorylation active site. The T-loop and T′-loop interact with each other to maintain a widened loop conformation. Since M792 is located in this key loop, it is likely that the M792I mutation damages the bicarbonate phosphorylation site of CPS1, consistent with its very low enzyme activity.

3.9. Binding of NCG to the E1034G mutant

Based on the crystal structure of CPS1, Glu1034 is located at the carbamate phosphorylation domain L3, approximately 50 Å away from the NAG binding site, and 27 Å away from the

phosphorylation sites in both domains L1 and L3 (Fig. 6A). The side-chain of Glu1034 forms hydrogen-bonding interactions with the side-chain of Arg814, which belongs to domain L1. The side-chain of Arg814 has intense hydrogen bonding interactions with the side-chains of the main-chain O of Gly911 and Glu821, and the side-chain of Gln916 (Fig. 6C). Since Glu1034 is located at the interface among the bicarbonate phosphorylation domain L1, integrating domain L2 and carbonate phosphorylation domain L3, the hydrogen bonding interaction network around Glu1034 may be important to stabilize the whole structure. However, the Glu1034Gly mutation seems to leave enough space to allow NCG to bind to this site, replace the function of Glu1034, and rebuild the hydrogen bonding interaction network to stabilize the enzyme. Our docking study indicated that NCG might bind to this cavity in a way that puts the side-chain of NCG in a similar position as the side-chain of Glu1034, allowing interaction with the side-chain of Arg814; its α-carboxyl group hydrogen bonds with the main-chain N of Leu1035 and the carbamyl group of NCG to interact with the main-chain oxygen atoms from the loop between Arg814 and Ile820 (Fig. 7). In contrast to NCG carbamyl, the methyl group of NAG is not amenable to this environment.

3.10. NCG plays a dual role for activation and stabilization of CPS1 to ameliorate the clinical condition of a patient with E1034G mutation

In our recent experiment of a 3-day trial of oral NCG in 5 patients with late-onset CPS1 deficiency, the patient with the E1034G mutation showed marked improvement in nitrogen metabolism and clinical condition with NCG administration [35]. Considering the stability of the E1034G mutant and the yield produced using the baculovirus/insect cell expression system, an *in vivo* abundance of the E1034G mutant protein that is similar to the wild-type enzyme would be expected. Even though the patient has a normal NAGS gene, it is likely that the amount of NAG in liver mitochondria would be insufficient to activate all the CPS1 enzyme molecules, which seems the case in normal healthy adults [31]. Thus, supplementation of NCG likely activated additional CPS1 molecules to augment the patient's ureagenesis. The cavity created in the protein by the replacement of a glutamate with glycine happens to allow NCG binding replacing the missing glutamate side chain, perhaps increasing protein stability. Taken together, our experiments indicate that NCG may have played a dual role here, activating more of the CPS1 E1034G mutant molecules and stabilizing them as a chaperon.

3.11. Negative response to NCG in a patient with M792I mutation

Enzymatic assay indicated that the recombinant M792I mutant has very low residual activity, likely due to the damaged bicarbonate phosphorylation site (see above). However, similar yields of the M792I mutant and wild-type CPS1 in insect cells suggest that this protein is stable. Similar thermal stability and protection by NAG plus ATP of the M792I and WT enzymes from elastase further confirm this assertion. Table 2 lists the liver biopsy derived relative abundance of wild-type CPS1 and M792I mutant, and also NAGS and OTC, demonstrating the a comparable *in vivo* abundance of the M792I mutant to WT CPS1. Our *in vitro* experiment demonstrated that the paradoxical reduction of the enzymatic activity in response to NCG could have happened due to relative over-abundance of NCG. Since the patient this mutation adhered to dietary protein restriction, it is unlikely that NAG was at a

higher than normal concentration. Thus, the negative response to NCG supplementation could be explained by supplementation of NCG.

4. Discussion

It is known that patients with NAGS deficiency respond remarkably well to NCG supplementation, which allows for normalization of blood ammonia and restoration of ureagenesis [9–11]. NCG, as a deacylase-resistant analog of NAG, binds the same site as NAG and replaced the function of NAG activating CPS1. We showed that supplementation of NCG may also benefit some patients with partial CPS1 deficiency [35]. However, the effect may vary from patient to patient. The biochemical properties of NCG, particularly its interchange with NAG, have not been studied in detail. We provide herein a possible explanation for the variable or even disparate effects of NCG supplementation in patients with CPS1 deficiency.

Our study suggests that NCG binds to the same site as NAG, activating CPS1, but in a suboptimal conformation. MgATP alone can protect WT CPS1 from thermal denaturation, but not from attack by elastase. However, a combination of MgATP and NAG or NCG can protect the protein from both thermal denaturation and elastase attack. Similar protection was observed for the E1034G and M792I CPS1 mutants, but NCG seems to work slightly better than NAG for the E1034G mutant. Auto-docking study suggested that NCG might in addition bind the cavity left by the E1034G mutation in a way that NAG cannot stabilize the mutant protein. In the matrix of liver mitochondria, MgATP is likely to be abundant under normal physiological conditions. However, NAG, generated by NAGS, may be insufficient to saturate all CPS1 molecules, especially under conditions of protein restriction. Therefore, in most situations, supplementation of NCG will not only activate more CPS1, but also help to stabilize the enzyme.

The potential effects of NCG supplementation in patients with different CPS1 mutations may vary in different conditions: First, if the mutant CPS1 does not have any residual activity or there is an insignificant amount of CPS1 enzyme, the supplementation of NCG will likely not have an effect. In a second scenario, if the mutant CPS1 has partial activity and the NAG produced from NAGS is not sufficient to activate all mutant CPS1 in the liver mitochondria, NCG supplementation will likely activate more enzymes and enhance ureagenesis. The current E1034G CPS1 mutant likely represents this scenario. A third possibility is that NAG is already abundant enough to saturate all or most CPS1 molecules. As mentioned above, this condition is unlikely, but is plausible. In this situation, supplementation of NCG will likely not help to increase ureagenesis, and in fact may decrease urea production because NCG might out-compete already bound NAG and activate the enzyme in a suboptimal conformation resulting in lower enzymatic activity. Possibly “relative overdosage” of NCG may potentially inhibit ureagenesis, which may have been the case with the patient homozygous for the M792I mutation. Therefore, it may be useful to try and work out the optimal dosage of NCG supplementation for patients with hyperammonemia depending on their respective genotype and biochemical phenotype.

Trials of NCG supplementation in patients with CPS1 deficiency are quite limited [35,49,50] and more are warranted, as are *in vitro* studies of recombinant CPS1 mutants. The newly developed baculovirus/insect cell expression system, which can produce a large amount of the recombinant CPS1 with desired mutations, provides a useful tool to evaluate the residual activity, protein yield and stability of CPS1 mutants. This tool has been successfully used to study the disease-causing roles and pathogenic mechanism of various mutations in CPS1 [36,38,51–54].

Even though the concentration of NCG in liver mitochondria of the subjects receiving 100 mg/kg/d of the drug is unknown, there seemed sufficient NCG to activate CPS1 and restore ureagenesis in subjects with negligible NAG. Our previous experiments demonstrated that a single dose of NCG administration to healthy young adults increased the formation of urea [31]. Therefore, in most cases, the NAG generated from NAGS in healthy adults must be insufficient to saturate all CPS1 molecules in the basal state. The above results are consistent with earlier observations that only 30–60% of CPS1 in mitochondria is in an active form in the basal state [55]. The NAG concentration in liver mitochondria of animals and human has been estimated to be 0.1–0.3 mM [5]. These values are close to the apparent K_a of 0.13 mM for NAG bound to purify CPS1. It seems that the biosynthetic capacity of NAGS is limited due to its low abundance (Table 2), and the level of NAG inside mitochondria is sufficient to activate only a portion of CPS1 allowing the supplementation of NCG to activate more.

Finally, since the affinity of NCG to CPS1 is 20–25 fold weaker than NAG, in order to allow NCG to work efficiently, its concentration should be in the range of 0.5–7.5 mM, in comparison to the NAG concentration inside mitochondria (0.03–0.30 mM). However, the peak concentration of NCG in plasma after oral administration of 100 mg/kg body weight in a healthy male is only about 0.015 mM [56]. It is still a mystery how NCG is taken up and concentrated within liver mitochondria to reach millimolar concentrations. Recently, a specific transporter for NCG uptake was identified [57]. More studies of NCG intestinal and hepatic uptake and its renal excretion are certainly needed. These studies illustrate the application of mutation-specific precision medicine approach to the treatment of a single gene disorder and the laboratory and clinical research tools available to help tailor treatment to a specific patient.

Acknowledgments

This work was supported by NIH grants R01DK064913 (MT), and the O'Malley Family Foundation.

References

1. Belanger M, Butterworth RF. Acute liver failure: a critical appraisal of available animal models. Metab Brain Dis. 2005; 20:409–423. [PubMed: 16382351]
2. Hall LM, Metzenberg RL, Cohen PP. Isolation and characterization of a naturally occurring cofactor of carbamyl phosphate biosynthesis. J Biol Chem. 1958; 230:1013–1021. [PubMed: 13525417]
3. Shigesada K, Aoyagi K, Tatibana M. Role of acetylglutamate in ureotelism. Variations in acetylglutamate level and its possible significance in control of urea synthesis in mammalian liver. Eur J Biochem. 1978; 85:385–391. [PubMed: 565715]
4. Shigesada K, Tatibana M. *N*-acetylglutamate synthetase from rat-liver mitochondria. Partial purification and catalytic properties. Eur J Biochem. 1978; 84:285–291. [PubMed: 25771]

5. Shigesada K, Tatibana M. Role of acetylglutamate in ureotelism. I. Occurrence and biosynthesis of acetylglutamate in mouse and rat tissues. J Biol Chem. 1971; 246:5588–5595. [PubMed: 5096083]
6. Shigesada K, Tatibana M. Enzymatic synthesis of acetylglutamate by mammalian liver preparations and its stimulation by arginine. Biochem Biophys Res Commun. 1971; 44:1117–1124. [PubMed: 5160402]
7. Grisolia S, Cohen PP. The catalytic role of carbamyl glutamate in citrulline biosynthesis. J Biol Chem. 1952; 198:561–571. [PubMed: 12999771]
8. Britton HG, Garcia-Espana A, Goya P, Rozas I, Rubio V. A structure-reactivity study of the binding of acetylglutamate to carbamoyl phosphate synthetase I. Eur J Biochem. 1990; 188:47–53. [PubMed: 2318203]
9. Caldovic L, Morizono H, Daikhin Y, Nissim I, McCarter RJ, Yudkoff M, Tuchman M. Restoration of ureagenesis in *N*-acetylglutamate synthase deficiency by *N*-carbamylglutamate. J Pediatr. 2004; 145:552–554. [PubMed: 15480384]
10. Tuchman M, Caldovic L, Daikhin Y, Horyn O, Nissim I, Nissim I, Korson M, Burton B, Yudkoff M. *N*-carbamylglutamate markedly enhances ureagenesis in *N*-acetylglutamate deficiency and propionic acidemia as measured by isotopic incorporation and blood biomarkers. Pediatr Res. 2008; 64:213–217. [PubMed: 18414145]
11. Heibel SK, Mew NA, Caldovic L, Daikhin Y, Yudkoff M, Tuchman M. *N*-carbamylglutamate enhancement of ureagenesis leads to discovery of a novel deleterious mutation in a newly defined enhancer of the NAGS gene and to effective therapy. Hum Mutat. 2011; 32:1153–1160. [PubMed: 21681857]
12. Mew NA, McCarter R, Daikhin Y, Nissim I, Yudkoff M, Tuchman M. *N*-carbamylglutamate augments ureagenesis and reduces ammonia and glutamine in propionic acidemia. Pediatrics. 2010; 126:e208–e214. [PubMed: 20566609]
13. Fernandez de Miguel S, Gimeno Diaz A, de Atauri R, Torres Peral F, Fernandez Carrion O, Ayestaran S. *N*-carbamyl glutamate treatment in hyperammoniemia decompensated propionic acidaemia. An Pediatr (Barc). 2009; 71:579–580. [PubMed: 19850540]
14. Filippi L, Gozzini E, Fiorini P, Malvagia S, la Marca G, Donati MA. *N*-carbamylglutamate in emergency management of hyperammonemia in neonatal acute onset propionic and methylmalonic aciduria. Neonatology. 2010; 97:286–290. [PubMed: 19887858]
15. Gebhardt B, Dittrich S, Parbel S, Vlaho S, Matsika O, Bohles H. *N*-carbamylglutamate protects patients with decompensated propionic aciduria from hyperammonaemia. J Inherit Metab Dis. 2005; 28:241–244. [PubMed: 15877213]
16. Jones S, Reed CA, Vijay S, Walter JH, Morris AA. *N*-carbamylglutamate for neonatal hyperammonaemia in propionic acidaemia. J Inherit Metab Dis. 2008; 31(Suppl 2):S219–S222. [PubMed: 18338235]
17. Levesque S, Lambert M, Karalis A, Melancon S, Russell L, Braverman N. Short-term outcome of propionic aciduria treated at presentation with *N*-carbamylglutamate: a retrospective review of four patients. JIMD Rep. 2012; 2:97–102. [PubMed: 23430860]
18. Schwahn BC, Pieterse L, Bisset WM, Galloway PG, Robinson PH. Biochemical efficacy of *N*-carbamylglutamate in neonatal severe hyperammonaemia due to propionic acidaemia. Eur J Pediatr. 2010; 169:133–134. [PubMed: 19680687]
19. Soyucen E, Demirci E, Aydin A. Outpatient treatment of propionic acidemia-associated hyperammonemia with *N*-carbamoyl-L-glutamate in an infant. Clin Ther. 2010; 32:710–713. [PubMed: 20435240]
20. Yap S, Leong HY, Abdul Aziz F, Hassim H, Sthaneshwar P, Teh SH, Abdullah IS, Ngu LH, Mohamed Z. *N*-Carbamylglutamate is an effective treatment for acute neonatal hyperammonaemia in a patient with methylmalonic aciduria neonatology. 2016; 109:303–307.
21. Gebhardt B, Vlaho S, Fischer D, Sewell A, Bohles H. *N*-carbamylglutamate enhances ammonia detoxification in a patient with decompensated methylmalonic aciduria. Mol Genet Metab. 2003; 79:303–304. [PubMed: 12948747]
22. Levrat V, Forest I, Fouilhoux A, Acquaviva C, Vianey-Saban C, Guffon N. Carglumic acid: an additional therapy in the treatment of organic acidurias with hyperammonemia? Orphanet J Rare Dis. 2008; 3:2. [PubMed: 18234091]

23. Kasapkara CS, Ezgu FS, Okur I, Tumer L, Biberoglu G, Hasanoglu A. *N*-carbamylglutamate treatment for acute neonatal hyperammonemia in isovaleric acidemia. Eur J Pediatr. 2011; 170:799–801. [PubMed: 21207059]
24. De Lonlay P, Benelli C, Fouque F, Ganguly A, Aral B, Dionisi-Vici C, Touati G, Heinrichs C, Rabier D, Kamoun P, Robert JJ, Stanley C, Saudubray JM. Hyperinsulinism and hyperammonemia syndrome: report of twelve unrelated patients. Pediatr Res. 2001; 50:353–357. [PubMed: 11518822]
25. Palladino AA, Stanley CA. The hyperinsulinism/hyperammonemia syndrome. Rev Endocr Metab Disord. 2010; 11:171–178. [PubMed: 20936362]
26. Huijmans JG, Duran M, de Klerk JB, Rovers MJ, Scholte HR. Functional hyperactivity of hepatic glutamate dehydrogenase as a cause of the hyperinsulinism/hyperammonemia syndrome: effect of treatment. Pediatrics. 2000; 106:596–600. [PubMed: 10969108]
27. Kasapkara CS, Kangin M, Tas FF, Topcu Y, Demir R, Ozbek MN. Unusual cause of hyperammonemia in two cases with short-term and long-term valproate therapy successfully treated by single dose carglumic acid. J Pediatr Neurosci. 2013; 8:250–252. [PubMed: 24470826]
28. Fernandez Colomer B, Rekarte Garcia S, Garcia Lopez JE, Perez Gonzalez C, Montes Granda M, Coto Cotallo GD. Valproate-induced hyperammonemic encephalopathy in a neonate: treatment with carglumic acid. An Pediatr (Barc). 2014; 81:251–255. [PubMed: 24315420]
29. Aires CC, van Cruchten A, Ijlst L, de Almeida IT, Duran M, Wanders RJ, Silva MF. New insights on the mechanisms of valproate-induced hyperammonemia: inhibition of hepatic *N*-acetylglutamate synthase activity by valproyl-CoA. J Hepatol. 2011; 55:426–434. [PubMed: 21147182]
30. van Karnebeek CD, Sly WS, Ross CJ, Salvarinova R, Yaplito-Lee J, Santra S, Shyr C, Horvath GA, Eydoux P, Lehman AM, Bernard V, Newlove T, Ukpeh H, Chakrapani A, Preece MA, Ball S, Pitt J, Vallance HD, Coulter-Mackie M, Nguyen H, Zhang LH, Bhavsar AP, Sinclair G, Waheed A, Wasserman WW, Stockler-Ipsiroglu S. Mitochondrial carbonic anhydrase VA deficiency resulting from CA5A alterations presents with hyperammonemia in early childhood. Am J Hum Genet. 2014; 94:453–461. [PubMed: 24530203]
31. Mew NA, Payan I, Daikhin Y, Nissim I, Nissim I, Tuchman M, Yudkoff M. Effects of a single dose of *N*-carbamylglutamate on the rate of ureagenesis. Mol Genet Metab. 2009; 98:325–330. [PubMed: 19660971]
32. Wu X, Wan D, Xie C, Li T, Huang R, Shu X, Ruan Z, Deng Z, Yin Y. Acute and subacute oral toxicological evaluations and mutagenicity of *N*-carbamylglutamate (NCG). Regul Toxicol Pharmacol. 2015; 73:296–302. [PubMed: 26188117]
33. Daniotti M, la Marca G, Fiorini P, Filippi L. New developments in the treatment of hyperammonemia: emerging use of carglumic acid. Int J Gen Med. 2011; 4:21–28. [PubMed: 21403788]
34. Haberle J, Boddaert N, Burlina A, Chakrapani A, Dixon M, Huemer M, Karall D, Martinelli D, Crespo PS, Santer R, Servais A, Valayannopoulos V, Lindner M, Rubio V, Dionisi-Vici C. Suggested guidelines for the diagnosis and management of urea cycle disorders. Orphanet J Rare Dis. 2012; 7:32. [PubMed: 22642880]
35. Mew NA, McCarter R, Daikhin Y, Lichter-Konecki U, Nissim I, Yudkoff M, Tuchman M. Augmenting ureagenesis in patients with partial carbamyl phosphate synthetase 1 deficiency with *N*-carbamyl-L-glutamate. J Pediatr. 2014; 165:401–403. e403. [PubMed: 24880889]
36. Diez-Fernandez C, Martinez AI, Pekkala S, Barcelona B, Perez-Arellano I, Guadalajara AM, Summar M, Cervera J, Rubio V. Molecular characterization of carbamoyl-phosphate synthetase (CPS1) deficiency using human recombinant CPS1 as a key tool. Hum Mutat. 2013; 34:1149–1159. [PubMed: 23649895]
37. Niesen FH, Berglund H, Vedadi M. The use of differential scanning fluorimetry to detect ligand interactions that promote protein stability. Nat Protoc. 2007; 2:2212–2221. [PubMed: 17853878]
38. Hu L, Diez-Fernandez C, Rufenacht V, Hismi BO, Unal O, Soyucen E, Coker M, Bayraktar BT, Gunduz M, Kiykim E, Olgac A, Perez-Tur J, Rubio V, Haberle J. Recurrence of carbamoyl phosphate synthetase 1 (CPS1) deficiency in Turkish patients: characterization of a founder mutation by use of recombinant CPS1 from insect cells expression. Mol Genet Metab. 2014; 113:267–273. [PubMed: 25410056]

39. Morris GM, Huey R, Lindstrom W, Sanner MF, Belew RK, Goodsell DS, Olson AJ. AutoDock4 and AutoDockTools4: automated docking with selective receptor flexibility. J Comput Chem. 2009; 30:2785–2791. [PubMed: 19399780]
40. Schuttelkopf AW, van Aalten DM. PRODRG: a tool for high-throughput crystallography of protein-ligand complexes. Acta Crystallogr D Biol Crystallogr. 2004; 60:1355–1363. [PubMed: 15272157]
41. Emsley P, Cowtan K. Coot: model-building tools for molecular graphics. Acta Crystallogr D Biol Crystallogr. 2004; 60:2126–2132. [PubMed: 15572765]
42. de Cima S, Polo LM, Diez-Fernandez C, Martinez AI, Cervera J, Fita I, Rubio V. Structure of human carbamoyl phosphate synthetase: deciphering the on/off switch of human ureagenesis. Sci Report. 2015; 5:16950.
43. Fahien LA, Schooler JM, Gehred GA, Cohen PP. Studies on the mechanism of action of acetylglutamate as an activator of carbamyl phosphate synthetase. J Biol Chem. 1964; 239:1935–1941. [PubMed: 14213380]
44. Lof C, Cohen M, Vermeulen LP, van Roermund CW, Wanders RJ, Meijer AJ. Properties of carbamoyl-phosphate synthetase (ammonia) in rat-liver mitochondria made permeable with toluene. Eur J Biochem. 1983; 135:251–258. [PubMed: 6884364]
45. Evans DR, Balon MA. Controlled proteolysis of ammonia-dependent carbamoyl-phosphate synthetase I from Syrian hamster liver. Biochim Biophys Acta. 1988; 953:185–196. [PubMed: 3258164]
46. Guadalajara AM, Rubio V, Grisolia S. Inactivation of carbamoyl phosphate synthetase (ammonia) by elastase as a probe to investigate binding of the substrates. Biochem Biophys Res Commun. 1983; 117:238–244. [PubMed: 6559079]
47. Marshall M, Fahien LA. Proteolysis as a probe of ligand-associated conformational changes in rat carbamyl phosphate synthetase I. Arch Biochem Biophys. 1988; 262:455–470. [PubMed: 3284464]
48. Powers-Lee SG, Corina K. Domain structure of rat liver carbamoyl phosphate synthetase I. J Biol Chem. 1986; 261:15349–15352. [PubMed: 3491068]
49. Kuchler G, Rabier D, Poggi-Travert F, Meyer-Gast D, Bardet J, Drouin V, Cadoudal M, Saudubray JM. Therapeutic use of carbamylglutamate in the case of carbamoyl-phosphate synthetase deficiency. J Inherit Metab Dis. 1996; 19:220–222. [PubMed: 8739970]
50. Williams M, Huijmans JGM, van Diggelen OP, van der Low EJTM, de Klerk JBC, Haberle J. Carbamoyl phosphate synthetase I (CPS 1) deficiency: treatment with carglumic acid (Carbaglu). J Inherit Metab Dis. 2010; 33:S118.
51. Diez-Fernandez C, Gallego J, Haberle J, Cervera J, Rubio V. The study of carbamoyl phosphate synthetase 1 deficiency sheds light on the mechanism for switching on/off the urea cycle. J Genet Genomics. 2015; 42:249–260. [PubMed: 26059772]
52. Diez-Fernandez C, Hu L, Cervera J, Haberle J, Rubio V. Understanding carbamoyl phosphate synthetase (CPS1) deficiency by using the recombinantly purified human enzyme: effects of CPS1 mutations that concentrate in a central domain of unknown function. Mol Genet Metab. 2014; 112:123–132. [PubMed: 24813853]
53. Pekkala S, Martinez AI, Barcelona B, Gallego J, Bendala E, Yefimenko I, Rubio V, Cervera J. Structural insight on the control of urea synthesis: identification of the binding site for N-acetyl-L-glutamate, the essential allosteric activator of mitochondrial carbamoyl phosphate synthetase. Biochem J. 2009; 424:211–220. [PubMed: 19754428]
54. Pekkala S, Martinez AI, Barcelona B, Yefimenko I, Finckh U, Rubio V, Cervera J. Understanding carbamoyl-phosphate synthetase I (CPS1) deficiency by using expression studies and structure-based analysis. Hum Mutat. 2010; 31:801–808. [PubMed: 20578160]
55. Cheung CW, Raijman L. The regulation of carbamyl phosphate synthetase (ammonia) in rat liver mitochondria. Effects of acetylglutamate concentration and ATP translocation. J Biol Chem. 1980; 255:5051–5057. [PubMed: 6246096]
56. Sharma P, Shah PA, Sanyal M, Shrivastav PS. Challenges in optimizing sample preparation and LC-MS/MS conditions for the analysis of carglumic acid, an *N*-acetyl glutamate derivative in human plasma. Drug Test Anal. 2015; 7:763–772. [PubMed: 25677217]

57. Schwob E, Hagos Y, Burckhardt G, Burckhardt BC. Transporters involved in renal excretion of N-carbamoylglutamate, an orphan drug to treat inborn *n*-acetylglutamate synthase deficiency. Am J Physiol Ren Physiol. 2014; 307:F1373–F1379.

58. McReynolds JW, Crowley B, Mahoney MJ, Rosenberg LE. Autosomal recessive inheritance of human mitochondrial carbamyl phosphate synthetase deficiency. Am J Hum Genet. 1981; 33:345–353. [PubMed: 7246541]

59. Tuchman M, Holzknecht RA. Human hepatic *N*-acetylglutamate content and *N*-acetylglutamate synthase activity. Determination by stable isotope dilution. Biochem J. 1990; 271:325–329. [PubMed: 2241918]

60. Caldovic L, Lopez GY, Haskins N, Panglao M, Shi D, Morizono H, Tuchman M. Biochemical properties of recombinant human and mouse *N*-acetylglutamate synthase. Mol Genet Metab. 2006; 87:226–232. [PubMed: 16321554]

61. Morizono H, Tuchman M, Rajagopal BS, McCann MT, Listrom CD, Yuan X, Venugopal D, Barany G, Allewell NM. Expression, purification and kinetic characterization of wild-type human ornithine transcarbamylase and a recurrent mutant that produces ‘late onset’ hyperammonaemia. Biochem J. 1997; 322(Pt 2):625–631. [PubMed: 9065786]

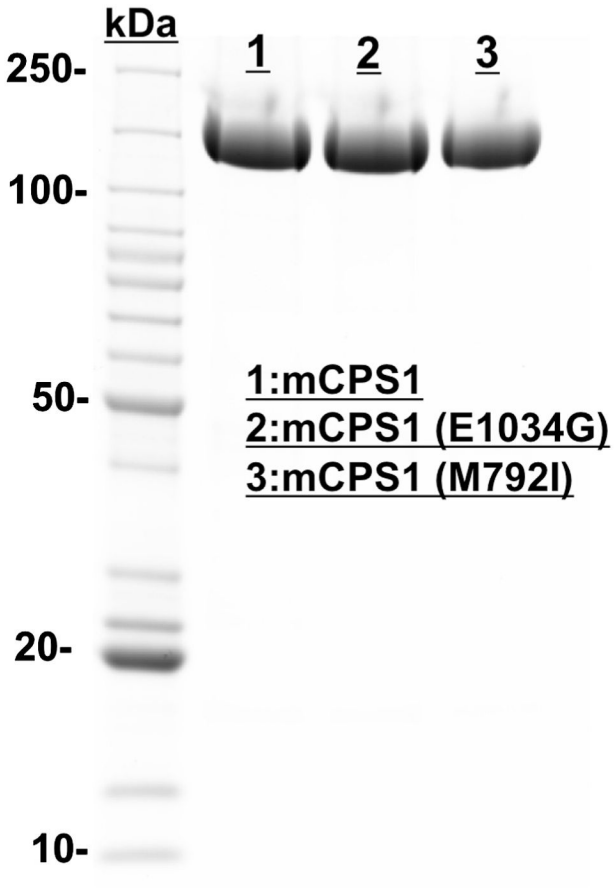

Fig. 1.

SDS/PAGE (Coomassie Blue staining, ~10 μg of total protein per lane) of purified wild-type mouse CPS1 and two mutants (E1034G and M792I) illustrating their expression levels. Lane1, recombinant wild-type mouse CPS1 (mCPS1); Lane 2, E1034G mouse CPS1 mutant; Lane 3, M792I mouse CPS1 mutant. (For interpretation of the references to colour in this figure legend, the reader is referred to the web version of this article.)

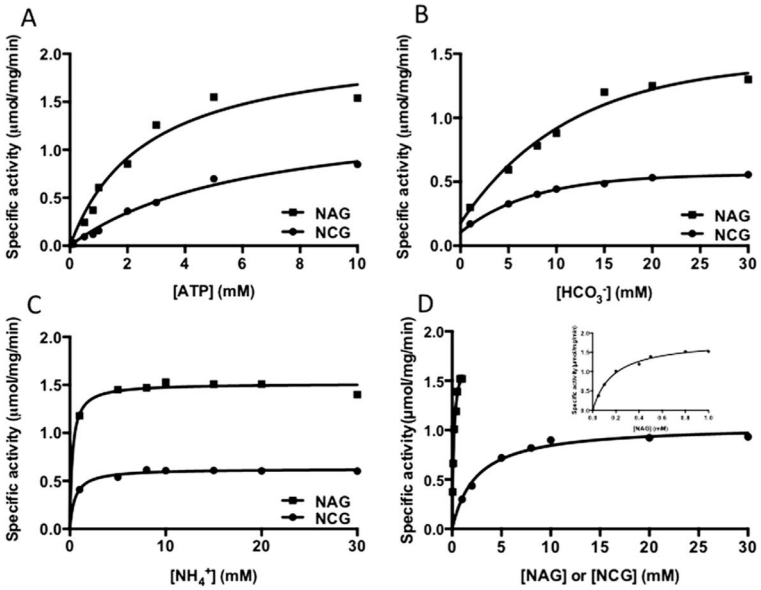

Fig. 2.

Comparison of biochemical properties of wild-type mouse CPS1 in the presence of NAG (1.0 mM) or NCG (10.0 mM). (A–C) Dependence of reaction velocity on the concentration of each substrate, ATP, bicarbonate and ammonium, respectively in the presence of NAG (square spots) or NCG (circle spots). (D) Dependence of reaction velocity on the concentration of NAG (square spots) and NCG (circle spots), illustrating their different affinity and maximum velocity. The inset is the enlargement of NAG titration curve.

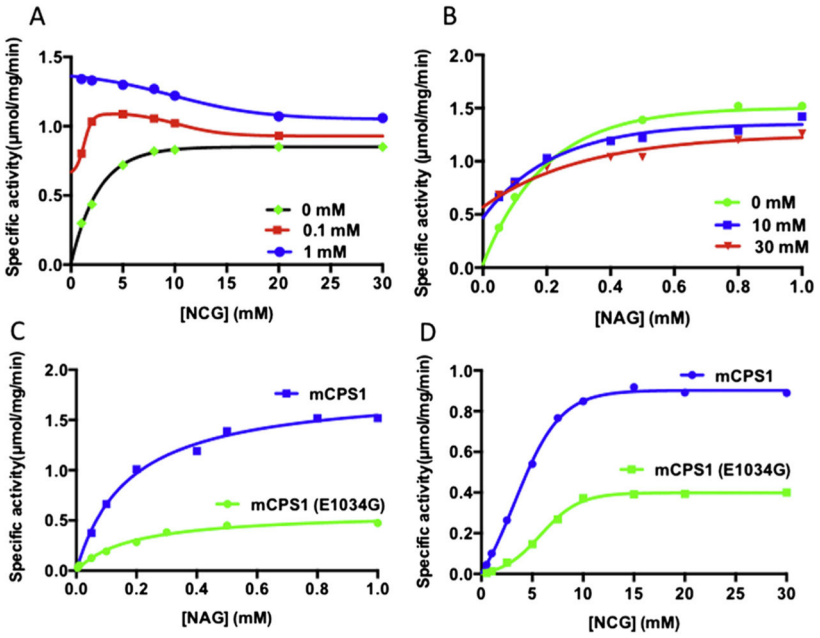

Fig. 3.

Competition between NAG and NCG. (A) Dependence of reaction velocity on the concentration of NCG in the absence (black curve) and presence of NAG in 0.1 mM (red curve) and 1.0 mM (blue curve) concentration. (B) Dependence of reaction velocity on the concentration of NAG in the absence (green curve) and presence of NCG in 10.0 mM (blue curve) and 30.0 mM (red curve). (C–D) Comparison of NAG (C) and NCG (D) titration between wild-type mouse CPS1 (blue curve) and E1034G CPS1 mutant (green curve).

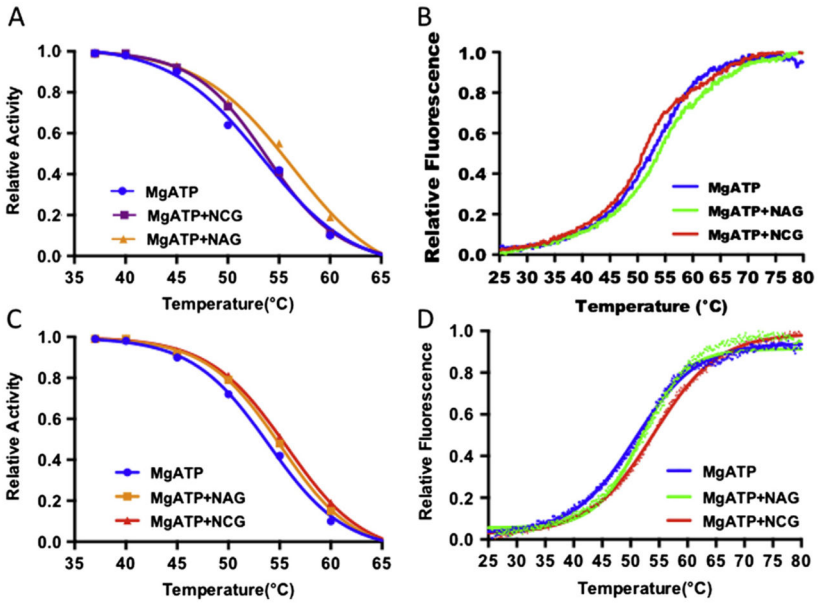

Fig. 4.

Thermal stability of wild-type CPS1 and E1034G mutant. (A) Remaining relative enzyme activity after incubation for 15 min at the indicated temperature for wild-type CPS1 in presence of MgATP (blue curve), MgATP + NAG (yellow curve) or MgATP + NCG (purple curve). (B) Relative fluorescence for wild-type CPS1 in presence of MgATP (blue curve), MgATP + NAG (green curve) or MgATP + NCG (brown curve) when temperature ramps from 298 K to 353 K. (C) Remaining relative enzyme activity after incubation for 15 min at the indicated temperature for the E1034G mutant in presence of MgATP (blue curve), MgATP + NAG (yellow curve) or MgATP + NCG (brown curve). (D) Relative fluorescence for the E1034G mutant in presence of MgATP (blue curve), MgATP + NAG (green curve) or MgATP + NCG (brown curve) when temperature ramps from 298 K to 353 K.

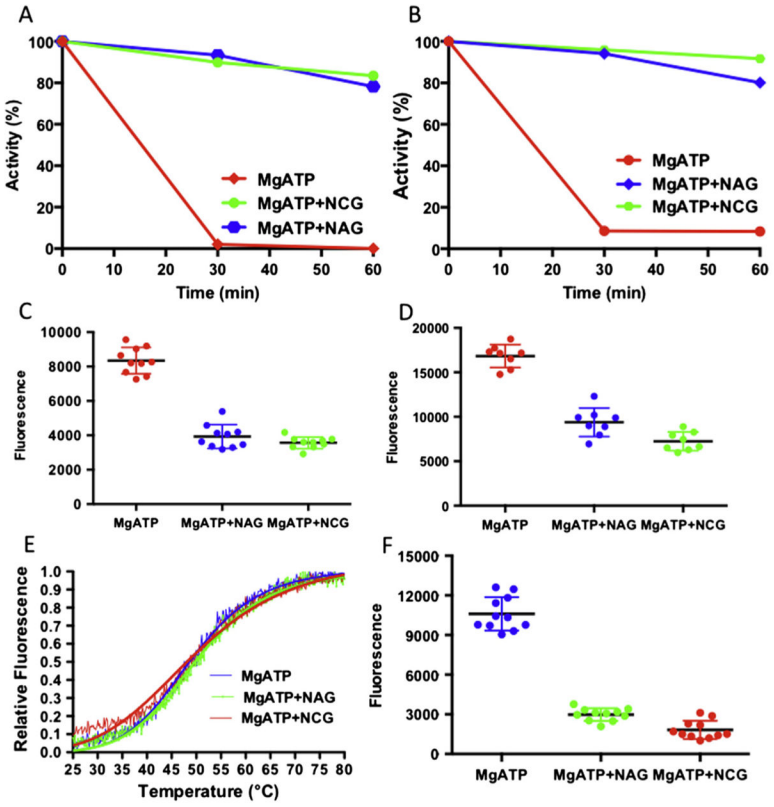

Fig. 5.

Protection of CPS1 in the presence of NAG or NCG with MgATP. (A–B) Remaining relative activity for the wild-type CPS1 (A) and E1034G mutant (B) after incubation with elastase for 40 and 60 min in the presence of MgATP (brown curve), MgATP + NAG (blue curve) or MgATP + NCG (green curve). (C–D) Fluorescence signals for the wild-type CPS1 (C) and E1034G mutant (D) after incubation with elatase for 10 min in the presence of MgATP (brown dots), MgATP + NAG (blue dots) or MgATP + NCG (green dots). (E) Relative fluorescence for the M792I mutant in presence of MgATP (blue curve), MgATP + NAG (green curve) or MgATP + NCG (red curve) when temperature ramps from 298 K to 353 K. (F) Fluorescence signals for the M792I mutant after incubation with elastase for 10 min in the presence of MgATP (blue dots), MgATP + NAG (green dots) or MgATP + NCG (red dots).

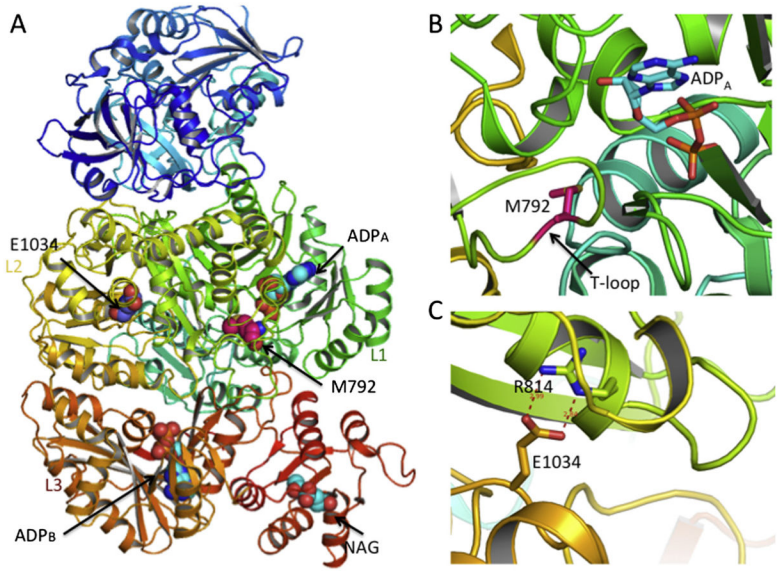

Fig. 6.

Locations of E1034G and M792I mutation in the CPS1 structure. (A) Ribbon diagram of the human CPS1 structure bound with NAG (sphere representation) and ADP showing the location of E1034 and M792. (B) Details of M792 site. The side-chain of M792 and the bound ADP are shown in sticks. (C) Details of E1034 site with hydrogen bonding interactions shown in dashed lines.

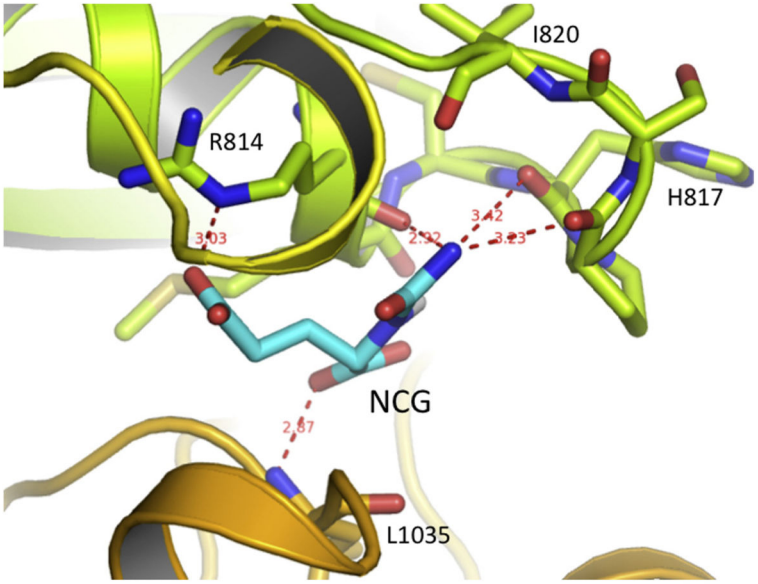

Fig. 7.

Proposed binding mode of NCG in the cavity created by E1034G mutation. The NCG is shown as magenta sticks and the hydrogen bonding interactions with the surrounding residues are shown in red dashed lines.

Table 1

Biochemical properties of mouse CPS1 in response to NCG and NAG.

Substrate or activator	K_m or K_a (mM)		V_{max} (μmol/min/mg)	
	NCG	NAG	NCG	NAG
ATP	6.3 ± 1.2	2.7 ± 0.6	1.4 ± 0.1	2.1 ± 0.2
Bicarbonate	5.2 ± 0.8	7.8 ± 0.6	0.56 ± 0.01	1.4 ± 0.1
Ammonium	0.88 ± 0.12	0.27 ± 0.35	0.64 ± 0.01	1.5 ± 0.1
NCG or NAG	2.23 ± 0.06	0.13 ± 0.05	0.92 ± 0.02	1.51 ± 0.05

Table 2

Relative abundance of CPS1, OTC and NAGS in liver.

	Enzymatic activity (μmol/min/mg)			
	CPS1		NAGS	OTC
	WT	M792I		
Liver	4.8×10^{-2} [58]	0.9×10^{-3} [35]	1.2×10^{-3} [59]	0.7 [58]
Recombinant protein	1.31 [54]	0.04	14.6 [60]	30 [61]
Relative abundance	3.7×10^{-2}	2.0×10^{-2}	8.2×10^{-5}	2.3×10^{-2}